

# TribeFlow: Mining & Predicting User Trajectories

Flavio Figueiredo<sup>1,2</sup>, Bruno Ribeiro<sup>3,4</sup>, Jussara Almeida<sup>2</sup>, Christos Faloutsos<sup>4</sup>

<sup>1</sup>UFCG - Brazil, <sup>2</sup>UFMG - Brazil, <sup>3</sup>Purdue University, <sup>4</sup>Carnegie Mellon University  
{flavio,jussara}@dcc.ufmg.br, ribeiro@cs.purdue.edu, christos@cs.cmu.edu

## ABSTRACT

Which song will Smith listen to next? Which restaurant will Alice go to tomorrow? Which product will John click next? These applications have in common the prediction of user trajectories that are in a constant state of flux over a hidden network (e.g. website links, geographic location). What users are doing now may be unrelated to what they will be doing in an hour from now. Mindful of these challenges we propose TribeFlow, a method designed to cope with the complex challenges of learning personalized predictive models of non-stationary, transient, and time-heterogeneous user trajectories. TribeFlow is a general method that can perform next product recommendation, next song recommendation, next location prediction, and general arbitrary-length user trajectory prediction without domain-specific knowledge. TribeFlow is more accurate and up to  $413\times$  faster than top competitors.

## Categories and Subject Descriptors

H.3.5 [Information Storage and Retrieval]: Online Information Services—*Web-based services*

## Keywords

User Trajectory Recommendation; Latent Environments;

## 1. INTRODUCTION

Web users are in a constant state of flux in their interactions with products, places, and services. User preferences and the environment that they navigate determine the sequence of items that users visit (links they click, songs they listen, businesses they visit). In this work we refer to the sequence of items visited by a user as the user's trajectory. Both the environment and user preferences affect such trajectories. The underlying navigation environment may change or vary over time: a website updates its design, a suburban user spends a weekend in the city. Similarly, user preferences may also vary or change over time: a user has different music preferences at work and at home, a user irreversibly moves from pop music to classic rock, a user prefers ethnic food on weekdays but will hit all pizza places while in Chicago for the weekend. These result in user trajectories that over multiple time scales can be non-stationary (depend on wall clock times), transient (some visits are never repeated), and time-heterogeneous (user behavior changes over time); please refer to Section 5 for examples. Unfortunately, mining non-stationary, transient, and time-heterogeneous stochastic processes is a challenging task. It would be easier if trajectories were stationary (behavior is independent of wall clock times), ergodic (visits are infinitely repeated), and time-homogeneous (behavior does not change over time).

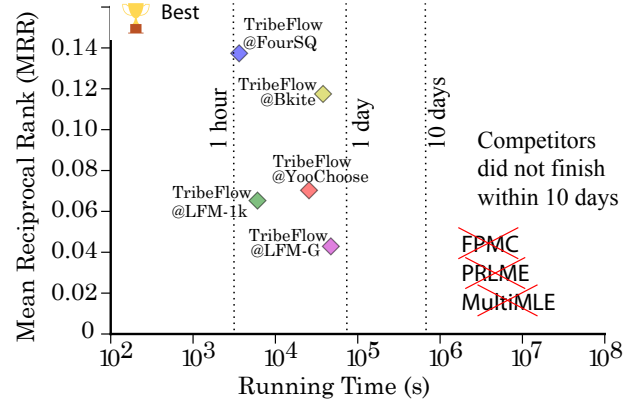


**Figure 1: TribeFlow is at least an order of magnitude faster than state-of-the-art methods for next-item predictions.**

In this work we propose TribeFlow to tackle the problem of mining and predicting user trajectories. TribeFlow takes as input a set of users and a sequence items they visit (user trajectories), including the timestamps of these visits if available, and outputs a model for personalized next-item prediction (or next  $n > 1$  items). TribeFlow can be readily applied to personalized trajectories from next check-in recommendations, to next song recommendations, to product recommendations. TribeFlow has no tunable parameters of importance, being parameter-free in all of our results. TribeFlow is highly parallel and nearly two orders of magnitude faster than the top state-of-the-art competitors. In order to be application-agnostic we ignore application-specific user and item features, including time-of-day effects, but these can be trivially incorporated into TribeFlow.

To illustrate the performance of TribeFlow consider Figure 1, where we seek to compare the Mean Reciprocal Rank (MRR) of TribeFlow over datasets with up to 1.6 million items and 86 million item visits (further details in Section 4) against that of state-of-the-art methods such as Multi-core Latent Markov Embedding (MultiLME) [40], personalized ranking LME (PRLME) [13], and Context-aware Ranking with Factorizing Personalized Markov Chains [45] (FPMC). Unfortunately, MultiLME, PRLME, and FPMC cannot finish any of these tasks in less than 10 days while for TribeFlow it takes between one and thirteen hours. In significantly sub-sampled versions of the same datasets we see that TribeFlow is always more accurate than its competitors, in fact, at least 23% more accurate.

TribeFlow works by decomposing potentially non-stationary, transient, time-heterogeneous user trajectories into *very* short sequences of random walks on latent environments that are stationary, ergodic,

and time-homogeneous. An intuitive way to understand TribeFlow is as follows. Random walks have been widely used for ranking items on *observed graph* topologies (e.g. PageRank-inspired approaches [5, 23, 24, 28, 42, 46, 57]); meanwhile, overlapping community detection algorithms [1, 34, 44, 63] also use *observed graphs* to infer latent weighted subgraphs. But *what if we were not given the environments (weighted graphs & time scales) but could see the output of a random surfer over them?* TribeFlow sees user trajectories and infers a set of latent environments (weighted item graphs and their time scales) that best describe user trajectories through short random walks over these environments; after the short walk users perform a weighted jump between environments; the jump allows TribeFlow to infer user preference of latent environments. Once the TribeFlow model infers the relationships between short trajectories and latent environments, we can give it any user history and current trajectory to infer a posterior over the latent environment that the user is currently surfing and, this way, perform accurate personalized next-item prediction using a random walk. In what follows we present a summary of our contributions.

### Our Contributions

- **(Accuracy).** In our datasets TribeFlow predictions are always more accurate than state-of-the-art methods. The state-of-the-art methods include Latent Markov Embedding (LME) of Chen et al. [10], Multi-LME of Moore et al. [40], PRLME of Feng et al. [13], and FPMC of Rendle et al. [45]. TribeFlow is also more accurate than an application of the time-varying latent factorization method (TM-LDA) of Wang et al. [60]. We also see why TribeFlow can better capture the latent space of user trajectories than state-of-the-art tensor decomposition methods such as Matsubara et al. [39].
- **(Parameter-free).** In all our results TribeFlow is used without parameter tuning. Because TribeFlow is a non-parametric hierarchical Bayesian method, it has a few parameters that are set as small constants and do not seem significantly affect the performance if there is enough data. The only parameter that affects performance ( $B \in \mathbb{Z}^+$  explained in the model description) is safely set to a small constant ( $B = 1$ ) in all of our results.
- **(Scalability).** TribeFlow uses a scalable parallel algorithm to infer model parameters from the data. TribeFlow is between  $48\times$  to  $413\times$  faster than our top competitors, including LME, PLME, PRLME, and FPMC. When available, we evaluated the performance of TribeFlow over the datasets originally used to develop the competing methods.
- **(Novelty).** TribeFlow provides a general framework to build upon (*random surfer over infinite latent environments*) and make application-specific personalized recommendation systems. The general concept of TribeFlow (illustrated in Figure 2) is described in detail in Section 3.

**Reproducibility.** Of separate interest is the reproducibility of our work. Both datasets and code that are not already publicly available can be found on our website<sup>1</sup>.

We now present the outline of this work. Section 2 reviews the related work. Section 3 describes the TribeFlow model. Section 4 presents our results on both small and reasonably-sized datasets of real-world user trajectories. Section 4 also compares TribeFlow both in terms of accuracy and speed against state-of-the-art and naive methods. Section 5 shows that TribeFlow has excellent sense-making capabilities. Finally, Section 6 presents our conclusions.

<sup>1</sup><http://github.com/flaviovdv/tribeflow> (Private repository until paper acceptance. Contact authors for access.)

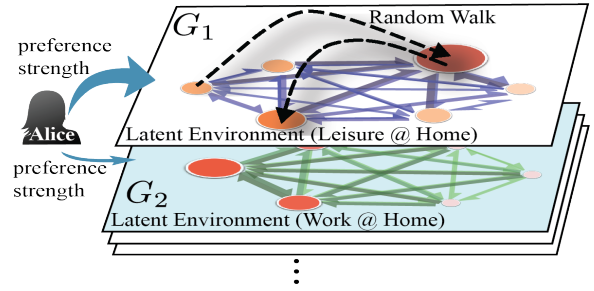


**Figure 2: (TribeFlow) Alice randomly chooses a (latent) environment (weighted item-item graph  $G_1$  and associated time scales) according to her preferences and surfs for a short time (two steps) before randomly jumping environments.**

## 2. RELATED WORK

How do we find a compact representation of the state space of network trajectories that allows easy-to-infer and accurate models? How can we learn non-stationary, transient, heterogeneous trajectories over this representation?

**Random Walk over Observed Networks.** The naive solution would be to simplify the state space of trajectories by merging nodes into communities via community detection algorithms [1, 44, 49, 63]. However, we do not have the underlying network. Rodriguez et al. [48] infers the underlying graph topology from epidemics but assumes a single underlying graph. In contrast, TribeFlow infers a possibly infinite set of latent environments (weighted graphs and inter-event times) from user trajectories without knowledge of the underlying network.

**Latent Markov Embedding.** Latent Markov Embedding (LME) [10, 11, 13, 58, 62] was recently proposed to tractably learn trajectories through a Markov chain whose states are projected user trajectories into Euclidean space. However, even with parallel optimizations [11] the method does not yet scaled beyond hundreds of thousands of users and items (as shown in Section 4.3). The LME method can be seen as one of the first practical approaches in the literature to jointly learn user memory & item preferences in trajectories. Wu et al. [62] present a factorization embedding adding user personalization to the LME predictions, called PLME, which is not parallel and suffers from a quadratic runtime. Very recently Feng et al. [13] relaxed some of the assumptions of PLME in order to focus only on rankings (thus, PRLME), making the quadratic learning algorithm become linear but not multi-core as Multi-LME.

**Factorizing Personalized Markov Chains.** Rendle et al. [45] proposes Factorizing Personalized Markov Chains (FPMC) to learn the stochastic process of user purchasing trajectories. FPMC predicts which item a customer would add next in his or her basket by reducing the state space of trajectories of each user into an unordered set (i.e., trajectory sequence is neglected). The resulting Markov model of each user transition in the space of items forms the slice of a tri-mode tensor which then is embedded into a lower dimensional space via a tensor decomposition. Similarly, Aizenberg et al. [2] performs a matrix factorization for embedding. Wang et al. [59] and Feng et al. [13] also make personalized factorization-style projections. Song et al. [56] and Hsu et al. [26] use singular value decomposition to embed the emission distribution of a HMM into a reproducing kernel Hilbert space, bypassing the problem of learning hidden states and the trajectory emission distribution. The work of Zheleva et al. [66] considers a highly application-dependent graphical model to explain user song plays through hidden taste and mood of songs but does not consider tra-

**Table 1: Comparison of Properties of State-of-art Methods.**

	MC MLE [35]	Gravity Model [53]	LDA/TM-LDA [21, 60]	LME/MultiLME [10, 40]	P(R)LME [13, 62]	FPMC [45]	Temporal Tensors	<b>TribeFlow (our method)</b>
General Approach	✓		✓	✓	✓	✓	✓	✓
Trajectory Model	✓			✓	✓	✓		✓
Personalized			✓		✓	✓	✓	✓
Multiple Time Scales								✓
Trajectory Memory	✓							✓
Sense Making	✓	✓	✓				✓	✓
Sub-Quadratic	✓	✓	✓		✓	✓	✓	✓
Scalable	✓	✓	✓				✓	✓

jectories. FPMC seems to be the most widely used method of this class that predicts next-items from unordered sets.

**Other Predictions over Unordered Sets.** Collaborative filtering methods can be broadly classified into two general approaches: memory-based [52] and item-based [37, 50]. In memory-based models [52] next item predictions are derived from the trajectory each user independently of other users. In item-based models [37, 50], next item predictions are based on the unordered trajectories of all users, which disregards the sequence of events in the trajectory. More general unordered set predictions use Collective Matrix Factorization [54]. Recently, Hierarchical Poisson Factorization of Gopalan et al. [20] deal with a different problem: item recommendation based on user ratings rather than user trajectories. Chaney et al. [9] extends the Gopalan et al. model for recommendations when network side information exists but also does not consider trajectories. The work of Wang et al. [60] uses a Latent Dirichlet Allocation-type embedding to capture latent topic transitions which we use to model trajectories in our comparisons (TM-LDA).

**Naive Methods.** Naive methods such as Gravity Model (GM) [53] are used to measure the average flow of users between items. Recently, Smith et al. [55] employs GMs to understand the flow of humans within a city. Galivanes et al. [18] employs GMs to understand Twitter user interactions. Note that GMs are application-dependent as they rely on a pre-defined distance function between items. Section 4.4 shows that TribeFlow is significantly more accurate than GM while retaining fast running times.

**Other Markov Chain Approaches.** A naive Markov Chain (MC) of the item-item transitions that are inferred via Maximum Likelihood Estimates (MLE) [35] does not provide enough flexibility to build a good predictive model. Markov Switching Models (MSMs) of Frohworth et al. [17] consider a different problem than ours: to identify time series in multiple speakers and objects speech and video application tasks. Fox et al. [15, 16] and Matsubara et al. [38] propose Bayesian generalizations of MSMs for a different problem: to segment video and audio. Liebman et al. [36] proposes a reinforcement learning (RL) method to predict song playlists. Liebman et al. tests the proposed RL method with only a few thousand users and hundreds of items in short sequences, significantly smaller than our smallest dataset and, thus, viable for comparison.

Table 1 compares TribeFlow with the strongest competitors in the literature for trajectory prediction and sense-making. TribeFlow is the only method that meets all criteria: general, personalized, multiple time scales, and scalable. Our inference algorithm is sub-quadratic in asymptotic runtime, as well as fully parallel. TribeFlow is the only approach that is accurate, general, and scalable.

### 3. THE TRIBEFLOW MODEL

TribeFlow models each user as a random suffer over latent environments. User trajectories are the outcome of a combination of latent user preferences and the latent environment that users are

exposed to in their navigation. We use a nonparametric model of short user trajectory sequences as steps of semi-Markov random walks into latent environments composed of random graphs and associated inter-event time distributions. Inter-event times between two consecutive items visited by a user. The model is learned via Bayesian inference. Our model is illustrated in Figure 2; user Alice jumps to a latent environment ( $\mathcal{M} = 1$ ) according to her environment preferences and performs two random walk steps ( $B = 1$ ) on graph  $G_{\mathcal{M}}$  with inter-event times associated to environment  $\mathcal{M}$ . After the two steps Alice randomly jumps to another latent environment of her preference.

Random walks on our latent environments are not to be confused with random walks on dynamic graphs. In the former the underlying graph topology and associated environment characteristics do not change once they are drawn from an unknown probability distribution while in the latter the graph structure is redrawn at each time step. In our applications probabilistic static environments seem like a better framework: a user with a given latent intent in mind (listen to heavy metal, eat spicy Indian food) at a given location (a webpage, a neighborhood) has item preferences (edge weights to songs, restaurants) similar to other like-minded users in the same network location. A random graph framework would be more accurate if webpages and restaurants randomly changed every time users made a choice. Our probabilistic environments are different from random graphs as the environment distribution is unknown and defines other characteristics such as the inter-event time distribution (simpler unidimensional examples of Markovian random walks on random environments with known distributions are given in Alexander et al. [3] and Hughes [27, Chapter 6]).

By construction, TribeFlow’s semi-Markov random walk generates ergodic, stationary, and time-homogeneous (E-S-Ho) trajectories. TribeFlow models potentially non-ergodic, transient, and time-heterogeneous user trajectories (Ne-T-He) as short sequences of E-S-Ho trajectories. By its nature E-S-Ho processes are generally easier to predict than Ne-T-He processes. And while a single user may not spend much time performing E-S-Ho transitions, other users will use the same E-S-Ho process which we believe allows us to infer it well.

#### 3.1 Detailed TribeFlow Description

The set of users ( $\mathcal{U}$ ) in TribeFlow can be agents such as people, bots, and cars. The set of items ( $\Omega$ ) can be anything: products, places, services, or websites. The latent environment  $\mathcal{M} = 1, 2, \dots$  is a latent weighted clique  $G_{\mathcal{M}} = (\Omega, E_{\mathcal{M}}) \sim \zeta(\mathbb{G})$  over the set of items  $\Omega$ . Edge weights in  $E_{\mathcal{M}}$  are drawn from a gamma distribution,  $w_{(\cdot, v)} = w_v \sim \text{Gamma}(\beta, 1), \forall v \in \Omega$ . In what follows we define the operator  $|\cdot|$  to be the size of a set and  $\otimes$  denotes the outer-product.

Each user  $u \in \mathcal{U}$  generates a “sequence trajectory” of length  $B + 1$  at the  $t$ -th visit,  $t \geq 1$ ,

$$(x_{u,t}, \dots, x_{u,t+B}) \in \Omega^{B+1}, B \geq 1,$$

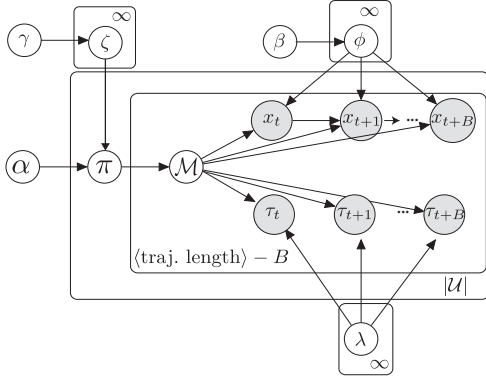


**Figure 3: The TribeFlow model of the user and the semi-Markov transition probability matrix mixture.**

before jumping to another environment  $\mathcal{M}'$  according to user preference distribution  $\pi_{\mathcal{M}'|u}$ . The entire trajectory  $x_{u,1}, x_{u,2}, \dots$  of user  $u \in \mathcal{U}$  is the concatenation of such sequences. Whether the trajectory of a user can be segmented into multiples of  $B$  is inconsequential to our inference problem as we infer posteriors over sliding windows.

The time between observations  $x_{u,t+k}$  and  $x_{u,t+k+1}$  is the  $k$ -th inter-event time  $\tau_{u,t+k}$ ,  $k = 0, \dots, B$ . Special care must be taken with the last event of a user, which does not have an inter-event (residence) time. The random walk over  $G_{\mathcal{M}}$  is modeled as a semi-Markov process with inter-event time  $\tau_{u,t} \sim \lambda(\mathcal{M})$  (a.k.a. holding or residence times). Note again that inter-event times depend on the latent environment that the walker observes.

We now define the transition probability matrix of our random walk over the random graph  $G_{\mathcal{M}}$ .

**THEOREM 3.1.** *The random walk over our environment can be defined by a semi-Markov chain  $\mathcal{M}$  with a random  $|\Omega| \times |\Omega|$  transition probability matrix distributed as*

$$\mathbf{P}_{\mathcal{M}} \sim (I - \text{diag}(\phi_{\mathcal{M}}))^{-1}(\phi_{\mathcal{M}} \otimes \phi_{\mathcal{M}} - \text{diag}(\phi_{\mathcal{M}}^2)), \quad (1)$$

where  $\text{diag}(\cdot)$  is a diagonal matrix and  $\phi_{\mathcal{M}} \sim \text{Dirichlet}(\cdot | \beta)$ . Semi-Markov chain  $\mathcal{M}$  is stationary, ergodic, and time-homogeneous with high probability if  $|\Omega| > 2$ .

**PROOF.** Without loss of generality we assume that the walker starts at  $u \in \Omega$ . The semi-Markov random walk with transition probability matrix  $\mathbf{P}_{\mathcal{M}}$  over  $G_{\mathcal{M}}$ ,  $\mathcal{M} \geq 1$ , sees edge weights  $w_v \sim \text{Gamma}(\beta, 1)$ ,  $\forall v \in \Omega \setminus \{u\}$ . The probability that the walk moves to  $v \neq u$  is  $w_v / S_{\neq u}$ , where  $S_{\neq u} = \sum_{j \in \Omega \setminus \{u\}} w_j$ . Let  $\mathbf{P}_{\mathcal{M}}(u, \Omega \setminus \{u\})$  denote the off-diagonal elements of the random walk transition probability matrix  $\mathbf{P}_{\mathcal{M}}$ . Because  $\{w_j\}_{j \in \Omega}$  are independent and Gamma distributed then

$$\mathbf{P}_{\mathcal{M}}(u, \Omega \setminus \{u\}) = (w_v / S_{\neq u})_{v \in \Omega \setminus \{u\}}$$

follows a Dirichlet distribution  $\text{Dirichlet}(\beta, \dots, \beta)$  [32, pp. 91]. Note that  $\mathbf{P}_{\mathcal{M}}(u, u) = 0$ . A little algebra gives Eq. (1). The chain is trivially stationary and time-homogeneous as transition probabilities do not change over time. We now show the chain is ergodic. Any state  $j \in \Omega$  is reachable from any state  $i \in \Omega$  as  $(\mathbf{P}_{\mathcal{M}})^n(i, j) > 0$  for some  $n \geq 1$  implying that the chain is recurrent [31, Theorem 5.1, pp. 66]. As  $|\Omega| < \infty$  the chain is positive recurrent. By construction  $G_1$  is connected and thus  $\mathbf{P}_{\mathcal{M}}$  is irreducible. For  $|\Omega| > 2$  the graph  $G_1$  is not bipartite and making the chain aperiodic. If a chain is irreducible, aperiodic, and positive recurrent, then it is ergodic [31, pp. 85].  $\square$

Note that the random walk does not have **revisits**,  $x_t \neq x_{t+1}, \forall t > 0$ . In the datasets we remove all revisits because re-consumption (repeated accesses to the same item) tends to be easy to predict [14], highly application-specific, and can be *decoupled entirely* from our problem via stochastic complementation using phase-type Markov chains with a single entry state such as the ones in Neuts [41], Robert and Le Boudec [47] and Kleinberg [33].

Gathering all elements together we obtain the model illustrated in Figure 3, which can be seen as a random surfer taking  $B$  steps over a latent graph  $G_{\mathcal{M}}$  and then randomly moving to a new environment as follows:

1. Draw  $\zeta \sim \text{GEM}(\gamma)$  according to a stick-breaking process.
2. For each user  $u \in \mathcal{U}$  sample  $\pi_{\mathcal{M}|u} \sim \text{Dirichlet}(\cdot | \alpha\zeta)$ .
3. Draw a semi-Markov random walk transition probability matrix  $\mathbf{P}_{\mathcal{M}} \sim (I - \text{diag}(\phi_{\mathcal{M}}))^{-1}(\phi_{\mathcal{M}} \otimes \phi_{\mathcal{M}} - \text{diag}(\phi_{\mathcal{M}}^2))$ , where  $\text{diag}(\cdot)$  is a diagonal matrix and  $\phi_{\mathcal{M}} \sim \text{Dirichlet}(\cdot | \beta)$ ,  $\mathcal{M} = 1, 2, \dots$
4. For a given user  $u$  each sequence burst  $(x_t, \dots, x_{t+B})_u$  with inter-event times  $(\tau_t, \dots, \tau_{t+B-1})$  is generated as follows:
  - (a) Draw a latent semi-Markov chain  $\mathcal{M} \sim \text{Multinomial}(\pi_{\mathcal{M}|u})$ .
  - (b) For  $k = 0, \dots, (B-1)$  select item  $x_{t+k}$  according to probability  $\mathbf{P}_{\mathcal{M}}(x_{t+k}, x_{t+k+1})$  and inter-event time  $\tau_{t+k'} \sim \lambda(\mathcal{M})$ ,  $k' = 0, \dots, B$ , where  $\lambda(\mathcal{M})$  is the inter-event time distribution of environment  $\mathcal{M}$ . Item  $x_1$  is drawn uniformly from  $\Omega$ .

In what follows we consider the problem of inferring the posteriors of TribeFlow from user trajectory data.

### 3.2 Inferring TribeFlow Model from Data

In what follows we tackle the problem of “reversing” the generative process to learn the latent environments and user preferences that when coupled with a random walk best correspond to user trajectories. Given a set of user trajectories  $\{(x_{u,1}, x_{u,2}, \dots) : \forall u \in \mathcal{U}\}$  from a set of items  $x_{u,t} \in \Omega$ ,  $t \geq 1$ , we infer:

- The number of environments  $K > 1$  from the data.
- Posteriors of a finite set of semi-Markov transition probability matrices  $\{\mathbf{P}_{\mathcal{M}} : \mathcal{M} = 1, \dots, K\}$  corresponding random walks over a finite set of graphs  $\{G_{\mathcal{M}} : \mathcal{M} = 1, \dots, K\}$ .
- Posteriors of a set of environment preferences of users  $\{\pi_{\mathcal{M}|u} : \forall u \in \mathcal{U}\}$ .

If the inter-event time distribution  $\lambda(\mathcal{M})$  comes of a known family we can also get posteriors for each environment  $\{\lambda(\mathcal{M}) : \mathcal{M} = 1, \dots, K\}$ . In our experiments, however, the best performing approach is a heuristic that does not entail a posterior distribution over inter-event times.

The probability that a user sees a sequence  $x_{u,t}, \dots, x_{u,t+B}$  with inter-arrival times  $\tau_{u,t}, \dots, \tau_{u,t+B}$  at environment  $\mathcal{M}$  is

$$P[x_{u,t}, \dots, x_{u,t+B}, \tau_{u,t}, \dots, \tau_{u,t+B} | \mathcal{M}] = \prod_{k=0}^{B-1} \mathbf{P}_{\mathcal{M}}(x_{u,t+k}, x_{u,t+k+1}) P[\tau_{u,t+k} | \mathcal{M}] P[\tau_{u,t+B} | \mathcal{M}],$$

with  $\mathbf{P}_{\mathcal{M}}$  as given in Eq. (1). The probability we observe such burst for user  $u \in \mathcal{U}$  is then

$$P[x_{u,t}, \dots, x_{u,t+B}, \tau_{u,t}, \dots, \tau_{u,t+B} | u] = \sum_{K=1}^{\infty} P[\zeta] P[\tau_{u,t+B} | \mathcal{M}] \pi_{\mathcal{M}|u} \alpha \zeta_u \times \prod_{k=0}^{B-1} \mathbf{P}_{\mathcal{M}}(x_{u,t+k}, x_{u,t+k+1}) P[\tau_{u,t+k} | \mathcal{M}], \quad (2)$$



where  $P[\mathcal{M}]$  is the stick-breaking prior over  $\mathcal{M}$ . Unrolling Eq. (1) into Eq. (2) we obtain the final equation that describes the trajectory burst probability

$$P[x_{u,t}, \dots, x_{u,t+B}, \tau_{u,t}, \dots, \tau_{u,t+B-1} | u] \propto \sum_{K=1}^{\infty} P[\zeta] P[\tau_{u,t+B} | \mathcal{M}] \pi_{\mathcal{M}|\alpha\zeta,u} \times \prod_{k=0}^{B-1} \frac{\phi_{\mathcal{M}}(x_{u,t+k+1})}{1 - \phi_{\mathcal{M}}(x_{u,t+k})} P[\tau_{u,t+k} | \mathcal{M}]. \quad (3)$$

We use collapsed Gibbs sampling to estimate the model posteriors as follows. Initially, given a sequence of size  $B + 1$ , we transform user trajectories into a set  $\mathcal{D}$  of tuples using a sliding window over the trajectories of each user. To exemplify, for  $B = 2$  each entry captures a tuple:

$$(u, x_{u,t}, x_{u,t+1}, x_{u,t+2}, \tau_{u,t}, \tau_{u,t+1}) \in \mathcal{D}, t \geq 1.$$

This tuple represents the user  $u$ , the sequence of items  $x_{u,t}, \dots, x_{u,t+B}$  and the inter-event times  $\tau_{u,t}, \dots, \tau_{u,t+B}$ . To infer TribeFlow posteriors we start with an initial estimate of the number of environments  $K$  and randomly (uniform) assign each tuple in  $\mathcal{D}$  to one environment.

After the initial assignment we count the number of tuples of each user  $u$ :  $n_u = \sum_{(u', \dots) \in \mathcal{D}} \mathbf{1}(u' = u)$ , where  $\mathbf{1}$  is the indicator function. We also count the number of times environment  $\mathcal{M}$  is assigned to a tuple from user  $u$ :  $e_{\mathcal{M},u}$ , as well as the joint count of items, at any position, and environments:  $c_{i,\mathcal{M}}$ , and count the number of tuples assigned to an environment  $\mathcal{M}$ :  $a_{\mathcal{M}}$ . Using some of these counts, and assuming for now that  $\zeta$  is given, we can infer [21]

$$\pi_{\mathcal{M}|\alpha\zeta,u} = \frac{e_{\mathcal{M},u} + \alpha\zeta(\mathcal{M})}{n_u + K\alpha\zeta(\mathcal{M})}, \quad \phi_{\mathcal{M}}(i) = \frac{c_{i,\mathcal{M}} + \beta}{a_{\mathcal{M}} + |\Omega|\beta}. \quad (4)$$

We then employ ECME [19] inference where: (1) the e-step consists of one pass over the entire dataset performing a Gibbs sampling update (in other terms, one iteration of the collapsed Gibbs sampler); (2) an m-step where the algorithm considers the probability of inter-event times according to the following procedure.

If the inter-event times of environments  $\mathcal{M} = 1, 2, \dots$  have a known probability law  $\lambda(\mathcal{M})$  we can include this law in our model with the appropriate priors (e.g. a Normal distribution with fixed variance can have a Normal prior), updating the distribution parameters in each m-step. If the law of  $\lambda(\mathcal{M})$  is unknown but inter-event times are observed, we use the empirical complementary cumulative distribution function (ECCDF) in the the following heuristic: We estimate the ECCDF of each  $\mathcal{M}$  based on the entries assigned to  $\mathcal{M}$  on the last e-step. If  $T_{\mathcal{M}}$  is the random variable that defines the inter-arrival at environment  $\mathcal{M} = 1, \dots$ . For inter-event time  $\tau_{u,t}$  the probability  $P[T_{\mathcal{M}} > \tau_{u,t}]$  given the current ECCDF is the number of entries whose observed inter-event times in  $\mathcal{M}$  are greater than  $\tau_{u,t}$ . Thus,  $\mathbf{1}(T_{\mathcal{M}} > \tau_{u,t})$  is a Bernoulli random variable [61] with parameter  $p = P[T_{\mathcal{M}} > \tau_{u,t}]$ . Adding a conjugate prior  $Beta(1, K - 1)$  to the Bernoulli gives the following predictive posterior [19]:

$$P[\tau_{u,t} | \mathcal{M}] \propto \frac{b_{>\tau_{u,t}, \mathcal{M}} + 1}{n_{\mathcal{M}} + K}, \quad (5)$$

where  $b_{>\tau_{u,t}, \mathcal{M}}$  is the number of tuples currently assigned to  $\mathcal{M}$  that have inter-arrival times greater than  $\tau_{u,t}$ . It is easy to see from Eq. (5) that transitions with a large inter-event time, when compared to others in  $\mathcal{M}$ , are less likely to have been generated by  $\mathcal{M}$  (the value of  $b_{>\tau_{u,t}}$  is smaller). This captures the intuition

that higher inter-event times may represent a change in user preferences, and is an integral part of how we learn  $\zeta$ , detailed below.

In our experiments the ECCDF heuristic consistently provides results than assuming Normal inter-event time distributions. Testing other application-specific inter-event time posteriors is of interest in more application-specialized future work.

We now infer  $K$ , the number of environments, by adapting the partial expectation (partial-e) and partial maximization (partial-m) hierarchical Dirichlet processes (HDP) heuristics of Bryant and Sudderth [7] as follows: (a) merge pairs of redundant environments when there is gain in the joint posterior probability of model & data; and (b) split environments based on their inter-event times by separating the 5% entries with highest inter-event time if there is a marginal gain in the posterior. The merge step (partial-e) is equivalent to the one described in [7]. Our split step (partial-m) splits a environment with high variance inter-event times into two environments with lower variance if the splitting improves the joint posterior probability of model & data.

**Parallel Learning:** Finally, the model can be fully trained in parallel using the approach described in Asuncion et al. [4]. Each processor learns the model on a subset of the dataset. After a processor performs an “E” and an “M” steps, another processor is chosen at random to synchronize the model state (merge count matrices of the Gibbs sampler and update ECCDF estimates), leaving them with the same count matrices and ECCDF estimates. After a fixed number of iterations, which we fix as 200, every processor meets a barrier and the partial-e and partial-m steps (merges and splits) are performed on a single master processor. After these partial-e and partial-m steps, the master-processor updates all slave processors and the parallel learning continues as previously described. The learning ends after a fixed number of iterations, which we set as 2,000 for the results in Section 4.

**Inference without Timestamps:** In a few of our datasets timestamps are not available. In these cases we only need to infer  $\mathbf{P}_{\mathcal{M}}$  and  $\pi_{\mathcal{M}|\alpha\zeta,u}$  without the need to take into account  $P[\tau_{t+k} | \mathcal{M}]$ . In our results we also take the opportunity to assume that the number of environments is fixed ( $\zeta(\mathcal{M}) = 1$ ) and infer the model posteriors using collapsed Gibbs sampling [21, 22, 29, 30, 38, 60, 64] employing Eqs. (3) and (4), updating the counts at each iteration (updating the posterior probabilities). We denote the latter simpler approach **TribeFlow-NT** (TribeFlow-NoTimestamps).

**Prior Parameters:** For all of our experiments, we fix prior parameters  $\alpha = 50/K$  and  $\beta = 0.001$ . Constant  $\gamma$  does not need to be stated explicitly. In the presence of large datasets changes to these values of priors are expected to have little impact on the outcome of Bayesian nonparametric models [19].

### 3.3 TribeFlow Predictions

In this work TribeFlow has two prediction tasks: **next-item** likelihood predictions and **ranking**. In what follows we describe how TribeFlow can be used for prediction tasks. The personalized predictive likelihood of user  $u \in \mathcal{U}$  for candidate next-item  $\tilde{x}_{t+1} \in \Omega$  is based on the last  $B$  items and inter-event times of the user. Observing that user  $u$  has chosen items  $x_{t-1}, \dots, x_{t-B}$  with inter-event times  $\tau_{t-1}, \dots, \tau_{t-B}$  gives a posterior probability that  $u$  is performing a random walk at latent environment  $\mathcal{M} \in \{1, \dots, K\}$ , where  $K$  is the learned number of latent environments, typically  $K < 10^3$  in our experiments. More precisely, the posterior probability that  $u \in \mathcal{U}$  is in environment  $\mathcal{M}$  after choosing items  $x_{t-1}, \dots, x_{t-B}$  with inter-event times  $\tau_{t-1}, \dots, \tau_{t-B}$  is

$$P[\mathcal{M} | u, x_{t-1}, \dots, x_{t-B}, \tau_{t-1}, \dots, \tau_{t-B}],$$

**Table 2: Summary of our datasets.**

	Users	Items	# Transitions	# Users	# Items	Inter-event Times	Timestamp Span
Last.FM-1k	User	Artist	10,132,959	992	348,156	Yes	Feb. 2005 to May 2009
Last.FM-Groups	User	Artist	86,798,741	15,235	1,672,735	Yes	Feb. 2005 to Aug. 2014
BrightKite	User	Venue	2,034,085	37,357	1,514,460	Yes	Apr. 2008 to Oct. 2010
FourSQ	User	Venue	453,429	191,061	87,345	Yes	Dec. 2012 to April 2014
YooChoose	Session	Product	19,721,515	6,756,575	96,094	Yes	Apr. 2014 to Sept. 2014
Yes	Playlist	Song	1,542,372	11,139	75,262	No	(No timestamps)

which yields the full likelihood

$$P[\tilde{x}_{t+1}|u, x_{t-1}, \dots, x_{t-B}, \tau_{t-1}, \dots, \tau_{t-B}] = \frac{\sum_{\mathcal{M}=1}^K \mathbf{P}_{\mathcal{M}}(x_t, \tilde{x}_{t+1}) P[\mathcal{M}|u, x_{t-1}, \dots, x_{t-B}, \tau_{t-1}, \dots, \tau_{t-B}]}{\sum_{\mathcal{M}=1}^K \mathbf{P}_{\mathcal{M}}(x_t, \tilde{x}_{t+1}) \prod_{k=1}^B \mathbf{P}_{\mathcal{M}}(x_{t-k}, x_{t-k+1}) P[\tau_{t-k}|\mathcal{M}] \pi_{\mathcal{M}|\alpha\zeta, u}} \quad (6)$$

The task of ranking the next items is easier and faster than predicting their likelihood. This is because we can speed up the predictions by not computing the denominator in eq. (6), as the denominator is the same for all values of  $\tilde{x}_{t+1} \in \Omega$ . Note that our rankings are personalized and take into account the inter-event times.

## 4. RESULTS

Previous sections introduce TribeFlow and explain how to infer its posteriors from data. We now turn our attention to compare TribeFlow against state-of-the-art approaches, solving the very same problems over some of the very same datasets (if publicly available) as their original papers. We also use larger publicly available dataset and one ever larger dataset that we collected for this study (available for download at our website). In what follows Section 4.2 contrasts TribeFlow against state-of-the-art methods for next-item ranking. Section 4.3 compares TribeFlow against methods that learn latent Markov chains and predict the likelihood of next items. Finally, Section 4.4 contrasts TribeFlow ability to predict average mean-field user flows against that of Gravity Model.

Although TribeFlow is able to predict not just the next-item but also the next  $n \geq 1$  items, our evaluations are based at next-item predictions because previous efforts mostly focused their evaluations on this task. We also consider the reconsumption problem (consecutive visits to the same item) treated in Figueiredo et al. [14] as a separate, likely easier, problem that can be dealt with via stochastic complementation as discussed in Section 3.1.

### 4.1 Datasets and Evaluation Setup

Our datasets encompass three broad range of applications: (a) location-based social networks (check-in datasets), (b) music streaming applications, and (c) user clicks on e-commerce websites. It is important to point out that recommendation engines and user interfaces influence user navigation and their trajectories. Such effects are considered to be an integral part of our predictive task. But TribeFlow can as easily learn pure user preferences if given a dataset with no environment bias (when that is possible).

Table 2 summarizes our datasets showing the number of users and items, the total number of  $x_t, x_{t+1}$  pairs visited all users (or transitions/trajectories when  $B = 1$ ) as well as the time span covered by the dataset. The set of items,  $\Omega$ , can be songs or artists on music datasets, venues on check-in data, and products on e-

commerce data. The set of users  $\mathcal{U}$  are individuals, a “playlist”, or a “browser session” as described next.

**Last.FM-Groups.** We collected this dataset (available for download). Last.FM is a music streaming service that aggregates data from various forms of digital music consumption, ranging from desktop/mobile media players to other streaming services. This dataset was crawled in August 2014, using the user groups<sup>2</sup> feature from Last.FM. We manually selected 15 groups of pop artists and two general interest groups<sup>3</sup>. For each group, we crawled the listening history of a subset of the users (the first users listed in the group)<sup>4</sup>.

**Last.FM-1k.** The second Last.FM dataset was collected in 2009 using snowball sampling by Celma et al. [8].

**BrightKite.** Brightkite is a location based social network (LBSN) where users share their current locations by check-ins. In this publicly available dataset, each items is a location where users are checks-in. Collected by Cho et al. [12].

**FourSQ** Our second LBSN dataset was gathered from FourSquare by Sarwt et al. [51] in 2014.

**YooChoose.** This dataset is comprised of user clicks on a large e-commerce business. Here, each users is captured by a session and the trajectories capture clicks on different products within the same session. As “users” are actually browser sessions, there is an upper-limit of 12 hours on recorded inter-event times of a single “user” (session).

**Yes.** Finally, the Yes dataset consists of song transitions (playlists) of popular broadcast (offline) radios in the United States. *This dataset does not provide explicit user information or timestamps.* However, we use TribeFlow-NT by defining the playlists as users and each song as an item. The Yes dataset was collected by Chen et al. [10, 11] to develop LME.

No filtering or trimming is done over the original data for the results shown in Figure 1. In our evaluation of trajectory predictions we divide the datasets into “past” ( $\mathcal{D}_{\text{past}}$ ) and “future” ( $\mathcal{D}_{\text{future}}$ ) by selecting a timestamp that splits the dataset into “the first 70% transitions” for “past” (training set) and the remaining 30% transitions in “future” (test set), with the exception of Yes that has no timestamps. This training and testing scenarios best represent real-life situations where the training is performed in batches over existing data. Note that some users will have trajectories confined in the “past” dataset while the trajectory of “new users” may be entirely placed in the “future” dataset. For the Yes data the training

<sup>2</sup>Pages in which the user discusses musical artists

<sup>3</sup>Active Users, Music Statistics, Briney Spears, The Strokes, Arctic Monkeys, Miley Cyrus, LMFAO, Katy Perry, Jay-Z, Kanye West, Lana Del Rey, Snoop Dogg, Madonna, Rihanna, Taylor Swift, Adele, and The Beatles

<sup>4</sup>We focus on the first (more active) users due to rate limits.

and testing sets are the ones pre-defined by Chen et al. [10, 11]. Due to limitations in scalability of state-of-the-art methods we also exploit subsamples of our larger datasets when necessary. These subsamples have the first 1000, 2000, 5000, 10000, 20000 and 100000 transitions ordered by timestamps of each dataset. We test TribeFlow’s robustness through these dataset subsamples.

**Setup:** Our tests run on a server with two 10-core Intel Xeon-E5 processors and 256 GB of RAM. In our tests we use fixed hyperparameters in TribeFlow, as discussed in Section 3; we also fix  $B = 1$ . We also test TribeFlow with  $B = 1, 2, 3, 4, 5$  finding that larger  $B$  improves accuracy at FourSQ, LFM-1k, LFM-Groups and reduces accuracy at Bkite and YooChoose (as explored later in this section). The conclusion is that performance depends on the dataset and, to make our results parameter-free, we fix  $B = 1$  for all results presented in this work.

## 4.2 TribeFlow for Next-item Ranking

Before we proceed to compare TribeFlow against competing approaches, it is important to note that in our comparisons **only TribeFlow can handle our larger datasets** as evidenced by Figure 1. All of our comparison against competing state-of-the-art methods are **performed over small or subsampled datasets due to the large runtimes of the competing methods**.

We start our discussion on ranking methods by focusing on the evaluation metric: the mean reciprocal rank. The reciprocal rank,  $RR$ , is the inverse of the position of the destination  $x_{t+1}$  on the ranking of *all* potential candidates in decreasing order. That is, if candidate,  $\tilde{x}_{t+1}$ , destinations *Big Brewery*, *Pizza Place*, and *Sandwich Shop* are ranked with probabilities 0.4, 0.5, and 0.1 respectively, and the *true* destination was *Big Brewery*, the reciprocal rank has value  $1/2$ . Using TribeFlow, the RR can be computed using Eq. (6) as follows (with  $B = 1$ ):

$$RR(x_{t+1}, x_t, \tau_t, u) = \frac{1}{\text{rank}(P[x_{t+1} | x_t, \tau_t, u])}. \quad (7)$$

Based on the reciprocal rank we can define a single metric for the whole test set, the mean reciprocal rank (MRR):

$$MRR(\mathcal{D}_{\text{future}}) = \frac{\sum_{x_{t+1}, x_t, \tau_t, u \in \mathcal{D}_{\text{future}}} RR(x_{t+1}, x_t, \tau_t, u)}{|\mathcal{D}_{\text{future}}|}. \quad (8)$$

**Impact of TribeFlow ECCDF and HDP heuristics.** Before comparing TribeFlow with competing approaches, we test if our heuristic of HDP expansion and contraction of latent environments & inter-event time ECCDF inference improves the quality of the predictions. That is, we run TribeFlow with and without the partial e- and m-steps described in Section 3. We train TribeFlow with an initial guess of  $K = 100$  environments and TribeFlow-NT (without partial e- and m-steps) with a maximum of 100 environments. We evaluate the MRR at our largest datasets: BrightKite, LastFM-Groups, LastFM-1k, and YooChoose, and one small dataset (FourSQ). At FourSQ and YooChoose both TribeFlow and TribeFlow-NT have the same accuracy, possibly because of lower quality timestamps: FourSQ user data appears subsampled *in time* and YooChoose browser sessions timeout at 12 hours. For the remaining datasets the MRR gains of TribeFlow over TribeFlow-NT are 7%, 45%, and 53%, for LastFM-1k, LastFM-Groups, and BrightKite, respectively. This shows that our partial e- and m-step heuristics can significantly improve the results.

**TribeFlow v.s. state-of-the-art.** We now turn to our comparison of TribeFlow against state-of-the-art competing ranking approaches. Our first competitor is Factorizing Personalized Markov Chain (FPMC) of Rendle et al. [45]. FPMC was initially proposed to predict the

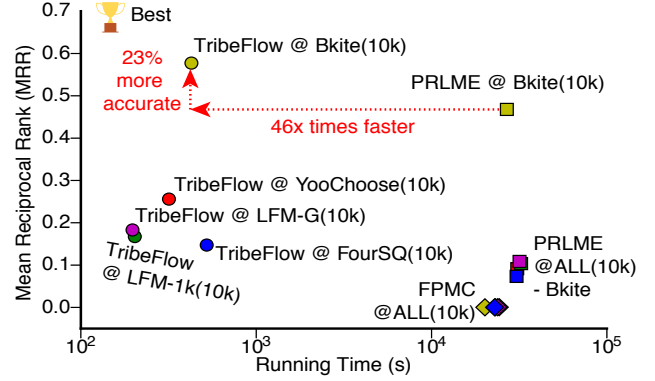


**Figure 4: TribeFlow again outperforms in ranking task (subsampled datasets with only  $10^4$  transitions).**

next object a user will insert into an online shopping basket. If we consider each source  $x_t$  as a size one shopping basket, FPMC can be used to rank the candidate items, or destinations  $\tilde{x}_{t+1}$ , that a user will consume next. Our second competitor is the best-performing Latent Markov Embedding (LME) method in our datasets: Personalized Ranking by Latent Markov Embedding (PRLME) of Feng et al. [13]. Inspired by Personalized Latent Markov Embedding [62] (PLME), the PRLME approach simplifies the LME/PLME to focus on rankings and not on extracting Markov embeddings, likely leading to the more accurate results we observed for PRLME.

Figure 4 presents the results of TribeFlow against FPMC and PRLME over datasets Bkite, FourSQ, LFM-Groups, LFM-1k, YooChoose subsampled to the first **10,000** transitions only due to scalability issues of FPMC and PRLME (even when limiting inference with 1000 stochastic gradient descent iterations). The figure shows the MRR scores (y-axis) against running times in log-scale (x-axis). Each point in the figure represents one method-dataset pair, while different datasets are represented by different colors. We label each point in order to help readability. The top-left corner of the figure indicates the best accuracy and shorter runtime. In these tests, as with all our tests, we use 70% of the initial user transitions to perform inference and the last 30% to test accuracy.

In Figure 4 we see that *TribeFlow is 23% more accurate and 46x times faster than the best result of PRLME*. In all cases TribeFlow is more accurate and faster than PRLME and FPMC, oftentimes TribeFlow is two orders of magnitude faster. This is surprising as TribeFlow runs parameter-free while PRLME and FPMC both optimize over a large parameter space to obtain their best results<sup>5</sup>. Our evaluation also considers a range of subsampled transitions in the datasets, from  $10^3$  to  $10^5$  transitions. The accuracy results are similar in all cases, with TribeFlow showing consistently more accurate results. Interestingly, using the results from the LastFM-Groups subsamples (1000, 5000, 10000, 20000,  $10^5$ ) using a simple linear regression reveals that it would take *over six years* to run PRLME and FPMC in the full LastFM-Groups dataset using our server. The minimum expected running time of PRLME/FPMC on a complete dataset is 14 days for the FourSQ dataset (the smallest dataset).

The results discussed so far consider only average measures of the effectiveness of the rankings produced by the methods. Going a step further, we also performed a Kolmogorov-Smirnov test between the distributions of reciprocal rank values obtained by TribeFlow and the competing methods. The results again clearly indicate that TribeFlow obtains larger RR values over all datasets ( $p < 0.001$ ), which is consistent the MRR results. Another aspect is the impact

<sup>5</sup>We perform a grid-search over parameters, testing 3 to 5 different values for each parameter of each method.

of the walker sequence length  $B$  on TribeFlow performance. We test TribeFlow with  $B = 1, 2, 3, 4, 5$  finding that larger  $B$  improves accuracy at FourSQ, LFM-1k, LFM-Groups and reduces accuracy at Bkite and YooChoose as shown in Figure 5. As the best choice of  $B$  is application dependent, we fixed  $B = 1$  in all our results.

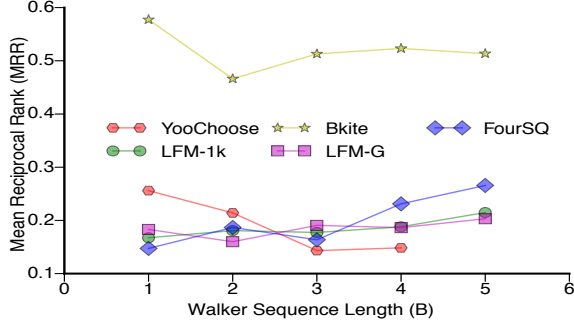


**Figure 5: Impact of walker sequence length  $B$  on TribeFlow performance over the largest datasets (YooChoose is limited to short sequence lengths).**

### 4.3 TribeFlow for Next-item Likelihood

In this section we compare the performance of TribeFlow against that of Latent Markov Embedding (LME) and Multi-LME [10, 11] in our smallest datasets, namely Yes and FourSQ. LME and even Multi-LME prohibits execution on anything but small datasets. Multi-LME computes  $P[x_{t+1} | x_t]_{\text{LME}}$  in Chen et al. [11] and thus to compare the methods we compute the transition matrix between items,  $\mathbf{P}^{(\text{TF})}$ , with TribeFlow as:

$$\mathbf{P}^{(\text{TF})} = \sum_{\mathcal{M}} \mathbf{P}_{\mathcal{M}} \sum_u \pi_{\mathcal{M}|\alpha\zeta, u} P[u], \quad (9)$$

where  $P[u] = (\text{no. tuples of user } u) / (\text{total no. tuples in dataset})$  and  $\mathbf{P}^{(\text{TF})}(x_t, x_{t+1}) = P[x_{t+1} | x_t]$ . We evaluate the accuracy of Multi-LME we use the same metric as Chen et al. [11] (the predictive log likelihood):

$$\text{PredLL}(\mathcal{D}_{\text{future}}) = \sum_{x_{t+1}, x_t \in \mathcal{D}_{\text{future}}} \log(P[x_{t+1} | x_t]), \quad (10)$$

where  $\mathcal{D}_{\text{future}}$  is the test set defined by Chen et al. [11] in the Yes dataset and 30% of the future transitions for other datasets.

*Adapting naive factorization approaches.* To compute  $P[x_{t+1} | x_t]$  one can also trivially adapt both Latent Dirichlet Allocation (LDA) [6] and Transition Matrix LDA (TM-LDA) [60] for the same task. LDA is trained with  $K$  latent factors and TM-LDA creates a  $(K, K)$  matrix capturing the probability of transitioning between a latent representation of  $x_t$  and the latent representation of  $x_{t+1}$ . Adaptation is done by exploiting the Bayesian graphical models of both models, re-arranging equations to compute  $(P[x_{t+1} | x_t])$ . We refer to these adaptations as LDA' and TM-LDA' for simplicity although they do not reflect the original intended applications of LDA and TM-LDA.

*Inference Procedure.* In our evaluations we use the fully parallelized Multi-LME implementation [11]<sup>6</sup>. The LDA' and TM-LDA' adaptations to our problem are trained using `scikit-learn` [43] which includes a fast/online [25] and parallelized implementation of these methods. While faster LDA' training methods do exist [65],

<sup>6</sup><http://www.cs.cornell.edu/People/tj/playlists/>

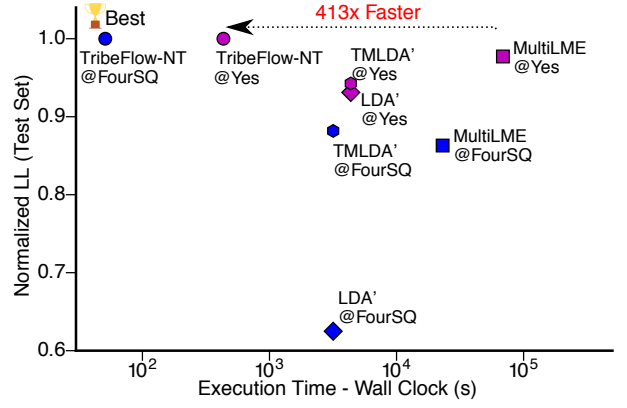


**Figure 6: TribeFlow outperforms competition in next-item predictive log-likelihood task (small dataset due to competitors).**

we preferred to make use of a mature software package. More importantly, due to the similar algorithm, TribeFlow can incorporate some of the heuristics used to speed-up LDA' approaches [65], an effort left as future work.

The Yes dataset of Chen et al. [10, 11] has no timestamps, thus we use TribeFlow-NT for this comparison instead of the more accurate general TribeFlow method. Each method was trained using different values of  $K$ , the number of latent environments ( $K \in \{10, 50, 25, 100\}$ ) on the Yes dataset and with  $K = 10$  on FourSQ because the original Multi-LME code has difficulties scaling to more factors on FourSQ.

*Results.* Figure 6 presents our results in the next-item predictive log-likelihood task using  $K = 100$  and  $K = 10$  on the Yes and FourSQ datasets. We get similar results for Yes with  $K \in \{10, 25, 50\}$ . For the sake of interpretability we normalize the predictive log likelihood of each method by the best result (always TribeFlow). Each point in the figure represents one method-dataset pair, while different datasets are represented by different colors. We labelled each point in order to help the interpretation of the results. With these settings, it is expected that the method that performs the best embedding is placed in the top-left corner of the figure (higher accuracy, lower runtime). The x-axis represents the execution time, whereas the y-axis represents the normalized likelihood.

In Figure 6 we clearly see that TribeFlow-NT is the best approach on both datasets. Compared to MultiLME TribeFlow-NT achieves a higher log-likelihood at a fraction of the runtime (speedups are up to 413 $\times$ ). As expected, TribeFlow-NT and MultiLME usually outperforms the LDA-based baselines since TribeFlow-NT and MultiLME were built to explicitly capture user trajectories. Interestingly, comparing the speed of TribeFlow and TribeFlow-NT in Figures 1 and 6 we see that for FourSQ TribeFlow-NT is one order of magnitude faster than TribeFlow but less accurate than TribeFlow.

### 4.4 TribeFlow Accurately Computes the Flows of Users Between Locations

TribeFlow outperforms the state-of-the-art methods in sophisticated tasks such as ranking and predictive next-item likelihoods. But what about a simpler task? Can TribeFlow outperform simple application-specific methods? In this section we compare TribeFlow against the Gravity Model (GM) for uncovering the average flows of users between two locations. The widely popular Gravity Model (GM) uses GPS coordinates and requires a pre-defined distance function, *dist*, capturing the proximity of locations around the globe. As in Smith et al. [55] and Garcia-Gavilanes et al. [18] we employ



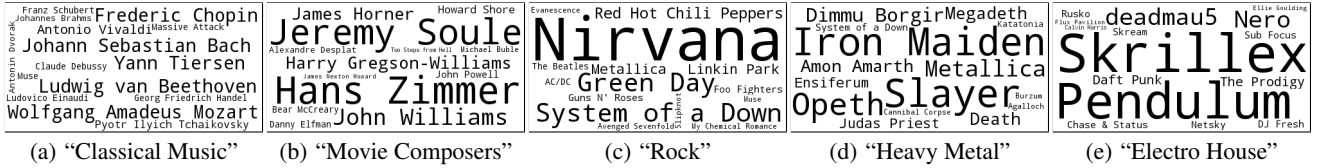


**Figure 7: (TribeFlow does well uncovering diverse environments even with strong data biases) Examples of popular items in latent TribeFlow environments in a dataset dominated by pop music fans (LFM-G).**

the distance on a sphere from the latitude and longitude coordinates of the venues in our LBSN datasets. The three parameters,  $\theta_1$ ,  $\theta_2$  and  $\theta_3$  of the distance are fitted using a Poisson regression that is known to lead to better results [53].

Our goal is to estimate  $f_{ds}$ , the flow of users going from location  $s \in \Omega$  to location  $d \in \Omega$ . Let  $n_d = \sum_{x_{t+1}, x_t \in \mathcal{D}_{\text{present}}} \mathbf{1}(x_{t+1} = d)$  denote the number of visits of all users to a destination  $d$  and  $r_s$  be the equivalent number of visits of all users to a source location  $s$ . GM captures the flows of users between the two locations  $f_{ds}$  as

$$\hat{f}_{ds}^{(\text{GM})} = \frac{r_s^{\theta_1} n_d^{\theta_2}}{\text{dist}(d, s)^{\theta_3}}.$$

TribeFlow can trivially estimate the flow  $\hat{f}_{ds}^{(\text{TF})}$  from Eq. (9). Since gravity models are limited to geolocated datasets (need GPS coordinates), we compare TribeFlow with GM on our FourSQ and Brightkite. Note that unlike GM, TribeFlow is application-agnostic and **does not** use GPS coordinates, albeit it would be straightforward to incorporate such application-specific features in the latent environments. Further, we opt to use TribeFlow-NT (instead of the more accurate TribeFlow method) because of its slightly faster running time, trading-off accuracy for speed. We infer the posteriors from TribeFlow-NT with  $K = 10$  environments. In this setting, the estimates of  $f_{ds}$  for both TribeFlow-NT and GM take less than 5 minutes. Both methods are evaluated using the mean absolute error (MAE):

$$\text{MAE} = \frac{\sum_{d,s} |f_{ds} - \hat{f}_{ds}^{(\cdot)}|}{|\{(d, s) | \forall x_{t+1}, x_t \in \mathcal{D}_{\text{future}} (d = x_{t+1} \wedge s = x_t)\}|}.$$

TribeFlow-NT significantly outperforms GM for geolocation flows with just a few ( $K = 10$ ) random environments and, unlike GM, without GPS coordinates. Specifically, GM achieves MAE results of 10.48 and 9.81 on the Bkite and FourSQ datasets, respectively. In contrast, TribeFlow-NT achieves **1.606** and **1.41** on Bkite and FourSQ, respectively. *The improvements of TribeFlow range from roughly 800% to 900% in mean absolute error.* Again, validating our results using the Kolmogorov-Smirnov test showed that TribeFlow-NT is statistically more accurate than GM ( $p < 0.001$ ).

Having seen that TribeFlow is faster and more accurate for next-item ranking and prediction than state-of-the-art methods, in the next section we discuss how TribeFlow can also be used for exploratory data analysis.

## 5. EXPLORATORY ANALYSIS

In this section we consider how TribeFlow can be used for sense-making in our datasets. Section 5.1 discusses the semantics of latent environments inferred by TribeFlow in our LastFM-Groups dataset, specially in the presence of non-stationary, transient, and time-heterogeneous user trajectories. Section 5.2 introduces latent environments inferred in the FourSQ dataset without GPS data. Finally, Section 5.3 discusses how TribeFlow compares with tensor decomposition approaches when uncovering meaningful patterns of user behavior from stationary user trajectory data.



**Figure 8: Latent flow environments inferred by TribeFlow without GPS information.**

### 5.1 Artist-to-Artist Transitions

Figure 7 shows five latent environments inferred by TribeFlow from the LastFM-Groups dataset. Each latent environment is represented as a word-cloud of the names of the top 15 artists in the environment ranked by the random walk steady-state probability at each environment. We cross-reference the top artists at each latent environment in Figures 7(a-e) with the AllMusic guide<sup>7</sup>, finding that the environments discovered are semantically meaningful. It is worth noting that users in the LastFM-Groups dataset are overwhelmingly declared fans of pop music (as described in Section 4.1), but even then, TribeFlow is able to extract the user interests of very diverse musical themes such as those depicted in Figure 7.

Taking a more in-depth look at the latent environment represented in Figure 7(a) shows a sequential user trajectory preference for songs related to “Classical Music”. Some of the main artists/composers in this environment are: Chopin, Bach, Beethoven and Mozart. The latent environment in Figure 7(b) shows composers of motion picture sound tracks. John Williams, for instance, compose soundtracks for popular movies such as Star Wars, Jaws, ET and Superman. The environment in Figure 7(c) represents popular rock bands such as Nirvana and Green Day, whereas the environment in Figure 7(d) represents heavy metal bands such as Iron Maiden and Slayer. Finally, the environment in Figure 7(e) represents *electro house* music being composed of groups such as Skrillex, Pendulum, deadmau5, and Nero.

### 5.2 Flow Semantics in Check-in Data

We now turn our attention to the Foursquare dataset. Environments in this dataset capture user trajectories between businesses. We want see whether TribeFlow infers semantically meaningful latent environments for check-in trajectory data. Interestingly, because TribeFlow **does not use GPS** features, TribeFlow can identify latent environments of “nearby” locations in any geometry.

Figure 8 shows the top-20 locations for two different latent environments inferred by TribeFlow. Each point in the figure is a latitude-longitude coordinate plotted on the world map from its GPS coordinate. Two latent environments best exemplify the sense-making abilities of TribeFlow. The first latent environment is represented by U.S. airports and seems to capture flows of U.S. domestic flights (including Hawaii). The second latent environment captures check-in trajectories of connections to/from Pacific-Asia-

<sup>7</sup><http://www.allmusic.com/>

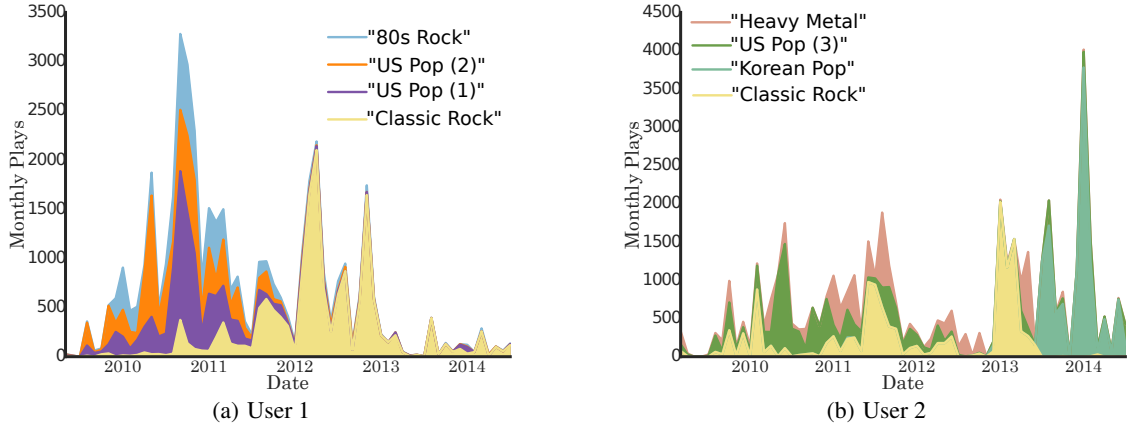


Figure 9: Example of Two Users From Last.FM-Groups

based airports. Also in this environment are major U.S./U.K. major hubs (JFK in New York City (NYC), LAX in Los Angeles and Heathrow in London) that connect to Pacific-Asia. Although omitted from the figure, TribeFlow also extracted environments based on user trajectories within cities including NYC, Miami and Atlanta. In these settings, check-ins are related to different places in these cities. This illustrates that TribeFlow latent environments can be a powerful tool for sense-making in large user trajectory datasets.

### 5.3 Transient User Trajectories

In this section we illustrate how TribeFlow can help us identify transient user trajectories (also showing that TribeFlow can cope well with the transience). To illustrate this, Figures 9(a,b) present the number of song plays (y-axis) over multiple years (x-axis) of two users from Last.FM-Groups broken down into the user’s four preferred latent environments. More precisely, the y-axis shows the cumulative sum of the song plays at a given month color-coded by the song’s most likely latent environment for that user,  $P[\mathcal{M}|u, x_t]$ .

As shown in the Figure 9(a), from 2010 until mid 2011 the user goes through a strong Pop phase – most representative (top) artists in the environment labeled “U.S. Pop (1)” are *Madonna*, *Nelly Furtado*, and *Alicia Keys*, and top artists in the “U.S. Pop (2)” environment are *Britney Spears*, *Leona Lewis*, and *Kelly Clarkson*. We also note some interest in 70-80’s Rock overtones – top artists being *Queen*, *Michael Jackson*, and *The Beatles*. After mid 2011 the user moves away from Pop artists towards a “Classic Rock” environment, with *The Beatles*, *Pink Floyd*, and *Nirvana* as top artists.

The user represented in Figure 9(b) also changes interest over time, most markedly from “Classic Rock” & “Heavy Metal” to “Korean Pop”. The two major take-aways are: (a) user trajectories are indeed transient (Figure 9); (b) users can show interests in the same latent environment at different points in time: User 1 Figure 9(a) shows strong “Classic Rock” environment preference between 2011-2012 while User 2 Figure 9(b) shows strong preference for the same environment between 2013-2014; and (c) TribeFlow can cope well with transient trajectories.

To provide further evidence in support TribeFlow’s ability to extract stationary, ergodic, and time-homogeneous behavior from user trajectories consider the following synthetic dataset. For comparison, we contrast TribeFlow with a state-of-the-art temporal tensor approach in the same scenario. This comparison sheds light into the reasons why tensor-factorization-based methods should have difficulty in extracting stationary, ergodic, and time-homogeneous behavior from user trajectory data.

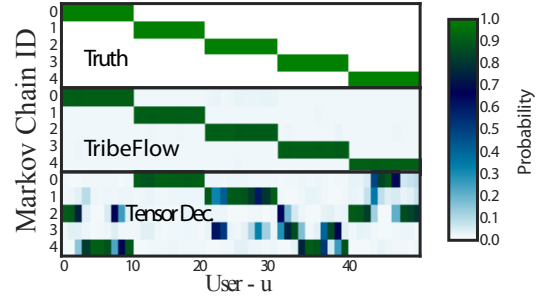


Figure 10: Comparison with Temporal Decomposition.

Our synthetic dataset has 50 users event assigned to one of five Markov chains. The Markov chains are used to create user trajectories. We model the popularity of items at each chain as a Lognormal distribution. Also, each environment has exponentially distributed inter-event times but timestamps are not recorded. We simulate a total of 5 days where and each user selects in average 100 items per day. We simulate users joining the system at different times (1 or 2 days apart).

Applying TribeFlow-NT to this synthetic data almost perfectly recovers user preferences of transition matrices as presented in Figure 10. TribeFlow should work even better if timestamps were available, but that would be an unfair comparison because of the extra feature. A state-of-the-art temporal decomposition method [39] (tensor with time mode) on the same data has trouble finding the ground truth (i.e., user ids 0 – 9 using Markov chain 0, user ids 10 – 19 using Markov chain 1, etc). Note that only TribeFlow is able to recover the different user trajectory preferences despite the asynchronous behavior of users. Clearly this type of tensor decomposition is meant to uncover only synchronized behavior as originally proposed by Matsubara et al. [39].

## 6. CONCLUSIONS

In this work we introduced TribeFlow, a general method to mine and predict user trajectories. TribeFlow decomposes non-stationary, transient, time-heterogeneous user trajectories into a small number of short random walks on latent random environments. The decomposed trajectories are stationary, erratic, and time-homogeneous in short time scales. User activity (e.g., listening to music, shopping for products online or checking-in different places in a city) is then captured by different latent environments inferred solely from observed user navigation patterns (e.g., listening to “classical music”, listening to “Brazilian Pop”, shopping for shoes, shopping for elec-

tronics, checking-in into airport fast-food venues, etc.). We summarize our major contributions as follows:

- **Accurate:** TribeFlow outperforms various baseline methods in three different tasks: extracting Markov embedding of user behavior, next-item prediction and capturing the flows of users between locations. Gains are up-to 900% depending on the dataset and task analyzed. TribeFlow is more accurate than Multi-LME by Chen et al. [11] when capturing the likelihood of trajectories on the very datasets used in Chen et al. [11] TribeFlow outperforms FPMC [45] and PRLME [13] in mean reciprocal rank (at least 23% gain), and beats the Gravity Model [53] when measuring the amount of times users transitions between geographic locations (up to 900% gain).
- **Scalable:** TribeFlow is at least tens and up to hundreds of times faster than state-of-the-art competitors even in relatively small datasets. If we consider the only other fully parallel competitor, MultiLME [11], TribeFlow is 413x faster and still more accurate.
- **Parameter-free:** TribeFlow has no tunable parameters unlike its state-of-the-art competitors.
- **Novelty:** TribeFlow provides a general framework to build upon (random surfer over infinite latent random environments) and make application-specific personalized recommendation systems.

## 7. REFERENCES

- [1] E. M. Airoldi, D. M. Blei, S. E. Fienberg, and E. P. Xing. Mixed Membership Stochastic Blockmodels. In *Proc. NIPS*, 2009.
- [2] N. Aizenberg, Y. Koren, and O. Somekh. Build your own music recommender by modeling internet radio streams. In *Proc. WWW. ACM*, 2012.
- [3] S. Alexander, J. Bernasconi, W. Schneider, and R. Orbach. Excitation dynamics in random one-dimensional systems. *Reviews of Modern Physics*, 53(2):175, 1981.
- [4] U. Asuncion, P. Smyth, and M. Welling. Asynchronous distributed estimation of topic models for document analysis. *Statistical Methodology*, 8, 2011.
- [5] L. Backstrom and J. Leskovec. Supervised random walks: Predicting and Recommending Links in Social Networks. In *Proc. WSDM*, 2011.
- [6] D. M. Blei, A. Y. Ng, and M. I. Jordan. Latent Dirichlet Allocation. *Journal of Machine Learning Research*, 3(4-5):993–1022, 2003.
- [7] M. Bryant and E. B. Sudderth. Truly Nonparametric Online Variational Inference for Hierarchical Dirichlet Processes. In *Proc. NIPS*, 2012.
- [8] O. Celma. *Music Recommendation and Discovery in the Long Tail*. Springer, 1 edition, 2010.
- [9] A. J. Chaney, D. M. Blei, and T. Eliassi-Rad. A probabilistic model for using social networks in personalized item recommendation. In *Proc. RecSys*, 2015.
- [10] S. Chen, J. L. Moore, D. Turnbull, and T. Joachims. Playlist prediction via metric embedding. In *Proc. KDD*, 2012.
- [11] S. Chen, J. Xu, and T. Joachims. Multi-space probabilistic sequence modeling. In *Proc. KDD*, 2013.
- [12] E. Cho, S. Myers, and J. Leskovec. Friendship and mobility: user movement in location-based social networks. In *Proc. KDD*, 2011.
- [13] S. Feng, X. Li, Y. Zeng, G. Cong, Y. M. Chee, and Q. Yuan. Personalized ranking metric embedding for next new POI recommendation. In *Proc. IJCAI*, 2015.
- [14] F. Figueiredo, J. M. Almeida, Y. Matsubara, B. Ribeiro, and C. Faloutsos. Revisit Behavior in Social Media: The Phoenix-R Model and Discoveries. In *Proc. PKDD/ECML*, 2014.
- [15] E. Fox, E. Sudderth, M. Jordan, and A. Willsky. Bayesian Nonparametric Methods for Learning Markov Switching Processes. *IEEE Signal Processing Magazine*, 27(6):43–54, Nov. 2010.
- [16] E. B. Fox, E. B. Sudderth, M. I. Jordan, and A. S. Willsky. Joint Modeling of Multiple Time Series via the Beta Process with Application to Motion Capture Segmentation. *Annals of Applied Statistics*, page 33, Nov. 2014.
- [17] S. Fröhlich-Schnatter and S. Kaufmann. Model-Based Clustering of Multiple Time Series. *Journal of Business & Economic Statistics*, 26(1):78–89, Jan. 2008.
- [18] R. García-Gavilanes, Y. Mejova, and D. Quercia. Twitter ain't without frontiers: economic, social, and cultural boundaries in international communication. In *Proc. CSCW*, 2014.
- [19] A. Gelman, J. B. Carlin, H. S. Stern, and D. B. Rubin. *Bayesian Data Analysis, Third Edition (Texts in Statistical Science)*. CRC Press, 2013.
- [20] P. Gopalan, J. M. Hofman, and D. M. Blei. Scalable Recommendation with Poisson Factorization. In *Proc. UAI*, 2015.
- [21] T. Griffiths. Gibbs sampling in the generative model of Latent Dirichlet Allocation. Technical report, Stanford University, 2002.
- [22] M. Harvey, I. Ruthven, and M. J. Carman. Improving social bookmark search using personalised latent variable language models. In *Proc. WSDM*, 2011.
- [23] T. H. Haveliwala. Topic-sensitive PageRank. In *Proc. WWW*, 2002.
- [24] T. H. Haveliwala. Topic-sensitive pagerank: A context-sensitive ranking algorithm for web search. *IEEE Transactions on Knowledge and Data Engineering*, 15(4):784–796, 2003.
- [25] M. D. Hoffman, D. M. Blei, and F. Bach. Online learning for latent dirichlet allocation. In *Proc. NIPS*, 2010.
- [26] D. Hsu, S. M. Kakade, and T. Zhang. A spectral algorithm for learning Hidden Markov Models. *Journal of Computer and System Sciences*, 78(5):1460–1480, Sept. 2012.
- [27] B. D. Hughes. *Random Walks and Random Environments*, volume 2. Clarendon; Oxford University Press, 1995.
- [28] G. Jeh and J. Widom. Scaling personalized web search. In *Proc. WWW*, 2003.
- [29] J.-H. Kang and K. Lerman. LA-CTR: A Limited Attention Collaborative Topic Regression for Social Media. In *Proc. AAAI*, 2013.
- [30] J.-H. Kang, K. Lerman, and L. Getoor. LA-LDA: A Limited Attention Model for Social Recommendation. In *Social Computing, Behavioral-Cultural Modeling and Prediction*. Springer, 2013.
- [31] S. Karlin and H. M. Taylor. Stochastic processes, 1975.
- [32] J. F. C. Kingman. *Poisson processes*, volume 3. Oxford university press, 1992.
- [33] J. Kleinberg. Bursty and Hierarchical Structure in Streams. In *Proc. ECML PKDD*, 2003.
- [34] P. N. Krivitsky, M. S. Handcock, A. E. Raftery, and P. D. Hoff. Representing degree distributions, clustering, and homophily in social networks with latent cluster random effects models. *Social Networks*, 31(3):204–213, July 2009.

- [35] D. A. Levin, Y. Peres, and E. L. Wilmer. *Markov Chains and Mixing Times*. AMS, 2008.
- [36] E. Liebman, M. Saar-Tsechansky, and P. Stone. DJ-MC: A Reinforcement-Learning Agent for Music Playlist Recommendation. In *Proc. AAMAS*, 2015.
- [37] H. Ma, H. Yang, M. R. Lyu, and I. King. SoRec : Social Recommendation Using Probabilistic Matrix Factorization. In *Proc. CIKM*, 2008.
- [38] Y. Matsubara, Y. Sakurai, and C. Faloutsos. AutoPlait: automatic mining of co-evolving time sequences. In *Proc. SIGMOD*, 2014.
- [39] Y. Matsubara, Y. Sakurai, C. Faloutsos, T. Iwata, and M. Yoshikawa. Fast mining and forecasting of complex time-stamped events. In *Proc. KDD*, 2012.
- [40] J. L. Moore, S. Chen, T. Joachims, and D. Turnbull. Taste Over Time: The Temporal Dynamics of User Preferences. In *Proc. ISMIR*, 2013.
- [41] M. F. Neuts. A versatile Markovian point process. *Journal of Applied Probability*, pages 764–779, 1979.
- [42] L. Page, S. Brin, R. Motwani, and T. Winograd. The pagerank citation ranking: bringing order to the web. Technical report, Stanford InfoLab, 1999.
- [43] F. Pedregosa, G. Varoquaux, A. Gramfort, V. Michel, B. Thirion, O. Grisel, M. Blondel, P. Prettenhofer, R. Weiss, V. Dubourg, J. Vanderplas, A. Passos, D. Cournapeau, M. Brucher, M. Perrot, and E. Duchesnay. Scikit-learn: Machine learning in Python. *Journal of Machine Learning Research*, 12:2825–2830, 2011.
- [44] S. Pool, F. Bonchi, and M. van Leeuwen. Description-Driven Community Detection. *ACM Transactions on Intelligent Systems and Technology*, 5(2):1–28, Apr. 2014.
- [45] S. Rendle, C. Freudenthaler, and L. Schmidt-Thieme. Factorizing personalized Markov chains for next-basket recommendation. In *Proc. WWW*, 2010.
- [46] M. Richardson and P. Domingos. The intelligent surfer: Probabilistic combination of link and content information in pagerank. In *Proc. NIPS*, 2001.
- [47] S. Robert and J.-Y. L. Boudet. On a Markov modulated chain exhibiting self-similarities over finite timescale. *Performance Evaluation*, 27-28:159–173, 1996.
- [48] M. G. Rodriguez, J. Leskovec, D. Balduzzi, and B. Schölkopf. Uncovering the structure and temporal dynamics of information propagation. *Netw. Sci.*, 2(01):26–65, 2014.
- [49] M. Rosvall and C. T. Bergstrom. Maps of random walks on complex networks reveal community structure. *PNAS*, 105(4):1118–1123, 2008.
- [50] R. Salakhutdinov and a. Mnih. Bayesian probabilistic matrix factorization using Markov chain Monte Carlo. In *Proc. ICML*, 2008.
- [51] M. Sarwat, J. J. Levandoski, A. Eldawy, and M. F. Mokbel. LARS\*: An Efficient and Scalable Location-Aware Recommender System. *IEEE Transactions on Knowledge and Data Engineering*, 26(6):1384–1399, 2014.
- [52] Y. Shi, M. Larson, and A. Hanjalic. Collaborative Filtering beyond the User-Item Matrix. *ACM Computing Surveys*, 47(1):1–45, May 2014.
- [53] J. M. C. S. Silva and S. Tenreiro. The Log of Gravity. *Review of Economics and Statistics*, 88(4):641–658, 2006.
- [54] A. P. Singh and G. J. Gordon. Relational learning via collective matrix factorization. In *Proc. KDD*, 2008.
- [55] C. Smith, D. Quercia, and L. Capra. Finger on the pulse: Identifying deprivation using transit flow analysis. In *Proc. CSCW*, 2013.
- [56] L. Song, B. Boots, and S. M. Siddiqi. Hilbert space embeddings of hidden Markov models. In *Proc. ICML*, 2010.
- [57] H. Tong, C. Faloutsos, and J. Y. Pan. Fast random walk with restart and its applications. In *Proc. ICDM*, 2006.
- [58] D. R. Turnbull, J. A. Zupnick, K. B. Stensland, A. R. Horwitz, A. J. Wolf, A. E. Spigel, S. P. Meyerhofer, and T. Joachims. Using Personalized Radio to Enhance Local Music Discovery. In *Proc. CHI*, 2014.
- [59] P. Wang, J. Guo, and Y. Lan. Modeling Retail Transaction Data for Personalized Shopping Recommendation. In *Proc. CIKM*, 2014.
- [60] Y. Wang, E. Agichtein, and M. Benzi. TM-LDA: Efficient Online Modeling of Latent Topic Transitions in Social Media. In *Proc. KDD*, 2012.
- [61] L. Wasserman. *All of Statistics : A Concise Course in Statistical Inference*. Springer Texts in Statistics, 2004.
- [62] X. Wu, Q. Liu, E. Chen, L. He, J. Lv, C. Cao, and G. Hu. Personalized next-song recommendation in online karaokes. In *Proc. RecSys*, 2013.
- [63] J. Yang, J. McAuley, and J. Leskovec. Community Detection in Networks with Node Attributes. In *Proc. ICDM*, 2013.
- [64] H. Yin, B. Cui, L. Chen, Z. Hu, and C. Zhang. Modeling Location-based User Rating Profiles for Personalized Recommendation. *ACM Transactions on Knowledge Discovery from Data*, To Appear, 2015.
- [65] H.-F. Yu, C.-J. Hsieh, H. Yun, S. Vishwanathan, and I. S. Dhillon. A Scalable Asynchronous Distributed Algorithm for Topic Modeling. In *Proc. WWW*, 2015.
- [66] E. Zheleva, J. Guiver, E. Mendes Rodrigues, and N. Milić-Frayling. Statistical models of music-listening sessions in social media. In *Proc. WWW*, 2010.